

IFUSP/P 512  
B.I.F. - USP

UNIVERSIDADE DE SÃO PAULO

# PUBLICAÇÕES

INSTITUTO DE FÍSICA  
CAIXA POSTAL 20516  
01498 - SÃO PAULO - SP  
BRASIL

IFUSP/P-512

B.I.F. - USP

OPTICAL AND THERMAL BLEACHING OF X-IRRADIATED  
BARIUM ALUMINOBORATE GLASSES

by

W.M. Pontuschka, S. Isotani, and A. Piccini  
Instituto de Física, Universidade de São Paulo

Janeiro/1985

OPTICAL AND THERMAL BLEACHING OF X-IRRADIATED  
BARIUM ALUMINOBORATE GLASSES

W.M. Pontuschka, S. Isotani, and A. Piccini  
Instituto de Física da Universidade de São Paulo,  
C. Postal 20.516, São Paulo, Brasil

New EPR studies of boron electron centers (BEC), boron-oxygen hole centers (BOHC) and interstitial atomic hydrogen centers ( $H_1^O$ ) in aluminoborate glasses X-irradiated at 77K are reported. Optical bleaching experiment suggests that protons ( $H_1^+$ ) are also present.

INTRODUCTION

Radiation damage in borate glasses induces several paramagnetic centers such as BEC, BOHC and  $H_1^O$ . The BEC was first studied by Griscom<sup>(1)</sup> in potassium borate glasses. As  $^{11}B$  nucleus is most abundant in nature (80.2%), three of the four transitions, due to hyperfine interaction between the trapped electron and the nuclear spin  $I = 3/2$ , are observed and easily recognised. It was proposed<sup>(1)</sup>, among other possibilities, that BEC is a center originated from the trapping of an electron at a vacant site of a non-bridging oxygen of a tetrahedral  $BO_4$  unit, forming a  $sp^3$  dangling bond.

Supported in part by FAPESP, CNPq and FINEP (Brasil).

Almost all X-irradiated borate glasses show a characteristic EPR line of 40 gauss width attributed to BOHC<sup>(2)</sup>. After some controversy<sup>(3)</sup>, it was generally accepted that this center is formed by the trapping of a hole on the  $\pi_z$  level of an oxygen bonded to a boron atom. Studies of these centers in glassy and crystalline compounds containing alkali and boron oxides proportional to 1:4, 1:3, 1:2 and 1:1, respectively, showed several characteristic structural units containing planar  $BO_3$  units and  $BO_4$  tetrahedra. In 1:1 compound the EPR line attributed to the BOHC has a structure of four lines, showing that the BOHC is localized in the neighbourhood of a bridging oxygen with substantial delocalization in the  $p_z$  orbital of the trigonal boron. In borate glasses containing 20% of alkaline oxides, the BOHC EPR line is structureless and it was assigned to a hole trapped a non-bridging oxygen.

The BOHC spectrum of 30at%BaO;50%B<sub>2</sub>O<sub>3</sub>;20%Al<sub>2</sub>O<sub>3</sub> X-irradiated at 77K, studied here, is shown in fig. 3.

Insert Figure 1

The kinetic studies of the EPR absorption lines of the atomic hydrogen center ( $H_1^O$ ) in barium aluminoborate glasses X irradiated at 77K have supported the assumption that they are trapped in  $B_nO_n$  ring structures<sup>(4)</sup>.

The growth curves of optical absorption in barium aluminoborate glasses doped with Ce  $\gamma$ -irradiated with  $^{60}Co$  showed to be a superposition of saturation exponentials<sup>(5)</sup>. This observation showed that the process of formation of BEC and BOHC is somewhat complex.

### EXPERIMENTAL PROCEDURES

The samples of barium aluminoborate glasses (30at% BaO; 60% B<sub>2</sub>O<sub>3</sub>; 10% Al<sub>2</sub>O<sub>3</sub>) were prepared and kindly furnished by Prof. A. Bishay of the Cairo American University. The details about the sample preparation, EPR measurements and temperature control conditions are explained elsewhere<sup>(4)</sup>. The X-irradiations were done using a Philips X-ray apparatus operating at 40 KV and 20mA. The samples were cooled by a cold finger within a cryostat at 10<sup>-5</sup> torr. The quartz window of this cryostat was located in front of a tungsten target tube. Care was taken in order to avoid sample heating above 110K during the transfer from the cold finger to the EPR spectrometer. The UV-irradiation was done with a 400W mercury lamp and the exposure to visible light with a Jarrell-Ash monochromator directed on the sample assembled in the EPR cavity.

The growth curves of the paramagnetic centers with X-irradiation times of 2, 4, 6, 8 and 24 hours, respectively, were obtained from average values determined from several samples. The error bars include the fluctuations among samples and measurements. After each measurement the sample was heated by 8 to 10 hours at 400°C in order to bleach the centers induced in the previous X-irradiation.

### RESULTS

Barium aluminoborate glasses, X-irradiated at 77K, exhibit the characteristic EPR spectrum shown in figures 2 and 3.

---

Insert Figures 2 and 3

---

In the figure 2 we see three of the four lines of BEC, a strong line of BOHC at the center of the spectrum and two additional lines of H<sub>1</sub><sup>O</sup> provenient from hydrogen impurity in the sample.

The detailed structure of the BOHC central line appear in figure 3. The nature of these lines is sensitive to the alkali content in the glass and a detailed description of this center is found in the literature<sup>(2)</sup>. The BOHC lines of our sample consist of a superposition of a structure of four lines ascribed to a hole trapped at a bridging oxygen and a single line attributed to a hole trapped at a non-bridging oxygen. On heating, the four-structured line is bleached before the single one, showing that the BOHC at bridging oxygen is less stable than the BOHC at non-bridging oxygen.

In figure 4 there are shown the growth curves of BEC and H<sub>1</sub><sup>O</sup>, averaged over four samples. The results were normalized in order to allow comparisons.

---

Insert Figure 4

---

As shown in figure 2, one of the four lines of BEC was obscured by the BOHC spectrum. This line can be observed by means of the suppression of the BOHC line introducing an impurity ion which is a good hole scavenger, such as Ag<sup>+</sup> or Ce<sup>3+</sup>. Both capture holes forming Ag<sup>++</sup> and Ce<sup>4+</sup> ions, respectively. The m<sub>I</sub> = + $\frac{1}{2}$  line of BEC can be seen in figure 5, at 3138 Gauss, in the spectrum of an X-irradiated barium aluminoborate glass containing

cerium impurity.

---

Insert Figure 5

---

With the gradual increase of temperature of annealing the spectra (see figure 6) show clearly the corresponding suppression of the BEC spectrum, remaining the more stable component, attributed to BOHC.

---

Insert Figure 6

---

The  $m_I = +\frac{1}{2}$  line is also visible in the spectrum of X-irradiated aluminoborate glass containing silver impurity (see figure 7).

---

Insert Figure 7

---

The samples X-irradiated at 77K, when heated in air, showed a blue luminescence. The EPR measurements showed that the BEC and  $H_i^O$  were bleached, remaining only the BOHC spectrum.

The annealing rates of BEC and  $H_i^O$  are not linearly correlated, as seen in the graphs of the respective isochronal decays (see figure 8). First, we see that the decay of BEC starts

---

Insert Figure 8

---

before than one of  $H_i^O$ , but with lower rate. At  $-60^\circ\text{C}$  all the  $H_i^O$  centers are bleached but the BEC concentration is still considerable.

The most interesting observation was the proof that the decay of BEC increases the concentration of  $H_i^O$ . We studied

this correlation inducing the decay of BEC by the exposure of the sample to visible light. In figure 9 it is shown the decay

---

Insert Figures 9a and 9b

---

of BEC ( $m_I = -\frac{1}{2}$ ) line and the corresponding growth of  $H_i^O$  by exposition to a mercury lamp at 113K. The practically linear growth above 60 minutes of exposition is due to the creation of  $H_i^O$  centers by the effect of the UV component of this light. In the same figure we see the growth curve of  $H_i^O$  with the exposition to UV component of the mercury lamp light of a non-irradiated sample. Subtracting the production of  $H_i^O$  by UV light, we see the increase of  $H_i^O$  due to the BEC bleaching (see figure 10).

---

Insert Figure 10

---

The decay rate of BEC is faster than the corresponding rate of increase of  $H_i^O$  due to the additional electron-hole recombinations.

We have examined the limit of light induced decay of BEC. We observed that even red light induces the decay of BEC, although at slower rate, with a measurable increase of  $H_i^O$  line intensity. On the other hand, only the UV component of light of the mercury lamp produces  $H_i^O$  in non-irradiated samples, in which case is followed by the production of BOHC.

The isothermal decay of BEC is plot in figure 11. The points are experimental data and the full line shows the results

---

Insert Figure 11

---

of an empirical adjustment using the empirical formula.

$$I(t) = I_0 t^{-b}$$

The values of  $I_0$  and  $b$  coefficients are shown in Table 1, together with the determination coefficient  $r^2$ .

---

Insert Table 1

---

The Arrhenius plot from these values is shown in figure 12 and the activation energy was obtained using the expression

$$E_{\text{BEC}} = \frac{\Delta \log b}{\Delta T^{-1}} (k/\log e) = (8.6 \pm 0.3) \times 10^{-21} \text{ J}$$

where  $E_{\text{BEC}}$  = BEC activation energy (eV) and  
 $k$  = Boltzmann's constant.

---

Insert Figure 12

---

We see that both  $I_0$  and  $b$  are not constant with temperature of the isothermal decay, showing the need of a more elaborated theoretical approach.

In addition to the study of the growth rate of BEC and  $H_1^0$  centers, we followed the evolution of the  $Fe^{3+}$  line at  $g = 4,1$ . The intensity of this line decays with the time of exposure of X-rays (see figure 13). Similar observation was reported earlier

---

Insert Figures 13a and 13b

---

by Bishay et al<sup>(6)</sup> and was assigned to the reduction of  $Fe^{3+}$  to  $Fe^{2+}$ .

The BOHC lines of the EPR spectra do not change at room temperature. These lines are bleached by heating at 400°C by 8h. During the bleaching it was observed an emission of orange light.

#### DISCUSSION AND CONCLUSIONS

The samples of barium aluminoborate glasses, when X-irradiated at 77 K, showed the formation of paramagnetic centers of the same kind of those observed in other borate glasses, i.e., BEC, BOHC,  $H_1^0$  and the reduction of  $Fe^{3+}$  with irradiation dose.

The BEC EPR spectrum observed is essentially the same described by Griscom et al<sup>(1)</sup> in potassium aluminoborate glasses. It consists of a hyperfine structure of four lines due to the interaction between a single electron trapped in a  $sp^3$  dangling orbital of boron and the  $^{11}\text{B}$  nucleus (80.2%) which has the nuclear spin  $I = 3/2$ . The BEC is stable at temperatures below 110 K.

The heating of BEC above this temperature produces strong blue luminescence.

The BOHC spectra observed in our samples have two components: (I) a structureless component of the line due to a hole trapped at a non-bridging oxygen<sup>(2)</sup>; (II) a quartet due to a hole trapped at a bridging oxygen<sup>(2)</sup>. Heating of BOHC at temperatures up to 400°C produces an orange luminescence.

In figure 14 we show a sketch of the mechanisms of

---

Insert Figure 14

---

formation of paramagnetic centers by X-irradiation at liquid nitrogen temperature in barium aluminoborate glass. The X-ray absorption induces the formation of electron-hole pairs. The analysis of the short time behaviour and the microscopic structure of these pairs is beyond the scope of the present work. We propose that the electrons and holes only can migrate throughout the sample if the electrons are excited to the conduction band and the holes injected in the valence band, otherwise they are always localized. This condition, obviously, is only satisfied when the sample is exposed to an irradiating source having photon energy at least equal to the band gap. The migration of holes is supported experimentally by the scavenge of holes by  $\text{Ag}^+$  and  $\text{Ce}^{3+}$  impurities.

The observed sites for the holes in the sample are the following: (a) non-bridging oxygen bonded to a boron atom<sup>(2)</sup>; (b) bridging oxygen between a planar  $\text{BO}_3$  and a tetrahedral  $\text{BO}_4$  structural unit<sup>(2)</sup>.

The BEC is probably a  $\text{sp}^3$  dangling orbital having a non-paired electron captured likely at an oxygen vacancy<sup>(1)</sup>.

The mechanisms of formation of  $\text{H}_1^{\text{O}}$  on the light of the present experimental data can be: (a) the photodissociation of hydroxyls bonded to boron atoms forming  $\text{BO}_3^-$  and  $\text{H}_1^+$  followed by the capture of an electron; (b) the capture of a photo-electron by hydroxyls bonded to boron atoms forming  $\text{BO}_3^-$  and  $\text{H}_1^{\text{O}}$ ; (c) the photodissociation of hydroxyls forming  $\text{BO}_3$  (BOHC) and  $\text{H}_1^{\text{O}}$ .

The reduction of  $\text{Fe}^{3+}$  into  $\text{Fe}^{2+}$  is assigned to the trapping of photo-electrons.

Figure 15 shows a sketch of the mechanism of formation

---

Insert Figure 15

---

of paramagnetic centers under UV light irradiation at 77K. In this process BEC is not formed.

Figure 16 shows a sketch of the effect of visible light

---

Insert Figure 16

---

on X-irradiated sample at liquid nitrogen temperature. The BEC is bleached even with red light showing that the BEC trap is shallow. The release of electrons from the BEC trap increases the concentration of  $\text{H}_1^{\text{O}}$  center. The blue luminescence was assigned to the electron-hole recombination at the BOHC site. The EPR spectrum of aluminoborate glass X-irradiated at 77K, exposed to 400 W mercury lamp for 1h at 113 K is shown in figure 17.

---

Insert Figure 17

---

The sketch shown in figure 18 represents the effects

---

Insert Figure 18

---

of heating to room temperature of X-irradiated samples. The BEC bleaching releases electrons which partially recombine with holes of the BOHC producing the emission of blue light. A fraction of these electrons react with  $\text{Fe}^{3+}$  forming  $\text{Fe}^{2+}$ .

It is shown in figure 19 a sketch of the effects of

---

Insert Figure 19

---

further heating of the X-irradiated sample to 400°C. The bleaching of BOHC release holes which are trapped by  $\text{Fe}^{2+}$  ions, which are oxidated to  $\text{Fe}^{3+}$ .

From the above discussions we conclude that Fe and OH impurities take part in the mechanisms of luminescence and irradiation effects in barium aluminoborate glasses.

#### REFERENCES

- (1) D.L. Griscom, "ESR Studies of Intrinsic Trapped-Electron Center in X-Irradiated Alkali Borate Glasses", *J. Chem. Phys.*, 55 [3] 1113-22 (1971).
- (2) D.L. Griscom, P.C. Taylor, D.A. Ware, and P.J. Bray, "ESR Studies of Lithium Borate Glasses and Compounds  $\gamma$ -Irradiated at 77K: Evidence for New Interpretation of Trapped-Hole Centers Associated with Boron", *J. Chem. Phys.*, 48 [11] 5158-73 (1968). P.C. Taylor and D. Griscom, "Toward a Unified Interpretation of ESR Trapped-Hole Centers in Irradiated Borate Compounds and Glasses", *J. Chem. Phys.*, 55 [7] 3610-11 (1971).
- (3) S. Lee and P.J. Bray, "Electron Spin Resonance Studies of Irradiated Glasses Containing Boron", *J. Chem. Phys.*, 39 [11] 2863-73 (1963). P. Beekenkamp, "Colour Centers in Borate, Phosphate and Borophosphate Glasses", *Philips Research Reports Suppl.*, [4] 117 pp. (1966). M.C.R. Symons, "Comments - Structure of Trapped-Hole Centers in  $\gamma$ -Irradiated Borate Glasses", *J. Chem. Phys.*, 53 [1] 468-9 (1970). D.L. Griscom, P.C. Taylor, and P.J. Bray, "Reply to - Structure of Trapped-Hole Centers in  $\gamma$ -Irradiated Borate Glasses", *J. Chem. Phys.*, 53 [1] 469-71 (1970).
- (4) W.M. Pontuschka, S. Isotani, A. Piccini, and N.V. Vugman, "EPR and Kinetic Studies of Hydrogen Centers in Aluminoborate Glasses", *J. Am. Ceramic Society*, 65 [10] 519-23 (1982).
- (5) P.W. Levy, P.L. Mattern, K. Lengweiler, and A.M. Bishay, "Studies on Nonmetals During Irradiation: V, Growth and Decay of Color Centers in Barium Aluminoborate Glasses Containing Cerium", *J. Am. Ceramic Society*, 57 [4] 176-81 (1974).

(6) A. Bishay, C. Quadros, and A. Piccini, "Cerium Centers in Glasses. Part I. ESR of Barium Aluminoborate Glasses Containing  $Ce^{3+}$ ", Phys. and Chem. of Glasses 15 [4] 109-12 (1974).

TABLE I - Constants of the expression  $I_{BEC} = I_{OBEC} t^{-b}$  calculated from experimental values.

T (K)	$I_{OBEC}$ (cm p-p)	b ( $min^{-1}$ )	$r^2$
183	16.39	0.077	0.99
203	14.61	0.098	0.99
213	12.29	0.10	0.99
233	8.86	0.13	0.99
253	8.14	0.19	0.996
273	4.06	0.21	0.97
293	2.65	0.27	0.98



## FIGURE CAPTIONS

Fig. 1 - Diborate-type structural unit in 30at% BaO; 60% B<sub>2</sub>O<sub>3</sub>; 10% Al<sub>2</sub>O<sub>3</sub> glass showing the likely sites for trapping holes. The proportion 1:2 corresponds to the local relative [alkaline oxide]:[boron oxide] molar concentrations.

Fig. 2 - EPR spectrum of 30at% BaO; 60% B<sub>2</sub>O<sub>3</sub>; 10% Al<sub>2</sub>O<sub>3</sub> glass X-irradiated at 77K, showing the characteristic BEC, BOHC and H<sub>i</sub><sup>o</sup> centers.

Fig. 3 - BOHC EPR spectrum of aluminoborate glass X-irradiated at 77 K.

Fig. 4 - Growth of H<sub>i</sub><sup>o</sup> and BEC EPR peak-to-peak amplitudes of the derivative of microwave absorption (I<sub>H<sub>i</sub><sup>o</sup></sub> and I<sub>BEC</sub>, respectively) in function of the X-rays exposure time (40 KV; 20 mA). Each error bar represents the distribution of measurements done with 4 samples. The exposure of 24 h was taken with only one sample.

Fig. 5 - EPR spectrum of 30at% BaO; 50% B<sub>2</sub>O<sub>3</sub>; 20% Al<sub>2</sub>O<sub>3</sub> glass containing 3.5at% of cerium, X-irradiated at 77K during 8 hours (40 K; 20 mA; tungsten target). The BOHC line is sufficiently weak in order to show clearly the m<sub>I</sub> = + $\frac{1}{2}$  BEC line, usually obscured in undoped aluminoborate glasses.

Fig. 6 - EPR spectra of 30at% BaO; 50% B<sub>2</sub>O<sub>3</sub>; 20% Al<sub>2</sub>O<sub>3</sub> glass containing 3.5at% of cerium, X-irradiated at 77K during 8 h (a) after annealing at 253 K for 3 h; (b) after further annealing at 295 K for 3 h.

Fig. 7 - EPR spectrum of 30at% BaO; 65% B<sub>2</sub>O<sub>3</sub>; 5% Al<sub>2</sub>O<sub>3</sub> containing 5at% of silver. The absence of BOHC line allows the observation of the usually obscured m<sub>I</sub> = + $\frac{1}{2}$  BEC line.

Fig. 8 - Isochronal annealing of BEC and H<sub>i</sub><sup>o</sup> centers in 30at% BaO; 60% B<sub>2</sub>O<sub>3</sub>; 10% Al<sub>2</sub>O<sub>3</sub> glass, X-irradiated at 77K during 8 h. The EPR signal amplitudes were obtained by measuring the height (cm peak-to-peak) of the derivative of absorption of BEC m<sub>I</sub> = - $\frac{1}{2}$  and H<sub>i</sub><sup>o</sup> (upper magnetic flux density line). The dashed lines were drawn in order to aid the reader's eye.

Fig. 9 - Effect of optical bleaching of 30at% BaO; 60% B<sub>2</sub>O<sub>3</sub>; 10% Al<sub>2</sub>O<sub>3</sub> glass, X-irradiated at 77K, on the BEC (m<sub>I</sub> = - $\frac{1}{2}$  line) and H<sub>i</sub><sup>o</sup> (upper magnetic flux density line) EPR line amplitudes in function of the time of exposure to the light source at 113K. The measurements were taken using (a) 250 W and (b) 400 W mercury lamps. The growth of H<sub>i</sub><sup>o</sup> at the bottom (■) was obtained from the UV-component of the 400 W mercury lamp, shed on the same sample when it was non-irradiated. The solid lines were drawn to aid the reader's eye. In this experiment it was used an optical-access cavity.

Fig. 10 - Growth curve of H<sub>i</sub><sup>o</sup> center after subtracting the growth of H<sub>i</sub><sup>o</sup> produced by the UV-component of the 400W mercury lamp (see Fig. 9b), compared with the decay curve of BEC. After 75 min of exposure, the curve above (★) is nearly saturated whereas the BEC (●) is almost completely bleached.

Fig. 11 - Isothermal annealing of BEC in 30at%BaO;60%B<sub>2</sub>O<sub>3</sub>;10%Al<sub>2</sub>O<sub>3</sub> glass X-irradiated at 77K. The solid lines represent the best fit to the empirical formula  $I(t) = I_0 t^{-b}$ .

Fig. 12 - Arrhenius plot  $b \times 1/T$  of the angular coefficients obtained from Fig. 11. The calculated activation energy is  $E_{\text{BEC}} = (8.6 \pm 0.3) \times 10^{-21}$  J.

Fig. 13 - a) EPR of  $g=4.1$  line of Fe<sup>3+</sup> in 30at%BaO;60%B<sub>2</sub>O<sub>3</sub>;10%Al<sub>2</sub>O<sub>3</sub> glass.  
b) Decay curve of the Fe<sup>3+</sup> EPR peak-to-peak amplitude in function of time of exposure to X-irradiation (40 KV; 20mA) at 77K.

Fig. 14 - Mechanisms of formation of paramagnetic centers in aluminoborate glasses X-irradiated at 77K. The Fe<sup>3+</sup> ions were partially reduced to Fe<sup>2+</sup>.

Fig. 15 - UV-irradiation effects in barium aluminoborate glass at liquid nitrogen temperature.

Fig. 16 - Visible light exposition effect on X-irradiated barium aluminoborate glass at liquid nitrogen temperature.

Fig. 17 - EPR spectrum of 30at%BaO;60%B<sub>2</sub>O<sub>3</sub>;10%Al<sub>2</sub>O<sub>3</sub> glass X-irradiated at 77K for 8h and bleached with the light of 400 W mercury lamp for 1h at 113K. The amplitude of H<sub>i</sub><sup>o</sup> lines has grown whereas the BEC spectrum was completely bleached. The central strong line is attributed to BOHC.

Fig. 18 - Effects of heating to room temperature of X-irradiated aluminoborate glasses.

Fig. 19 - Effects of heating X-irradiated aluminoborate glasses from room temperature to 400°C.

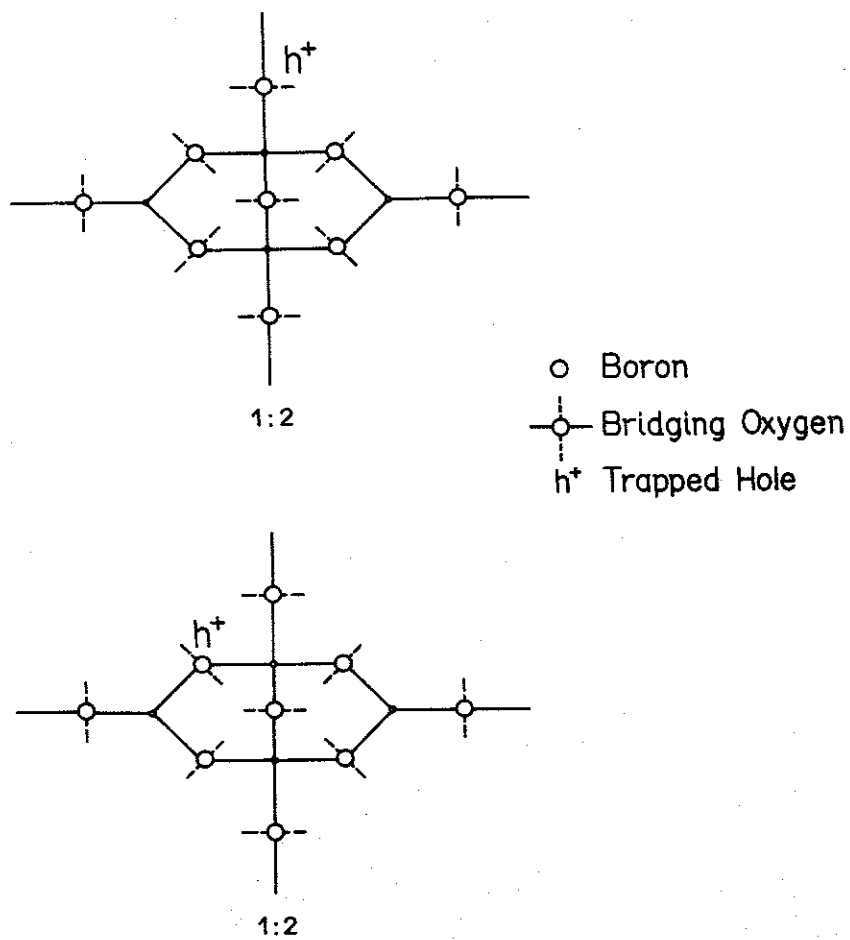


Fig. 1

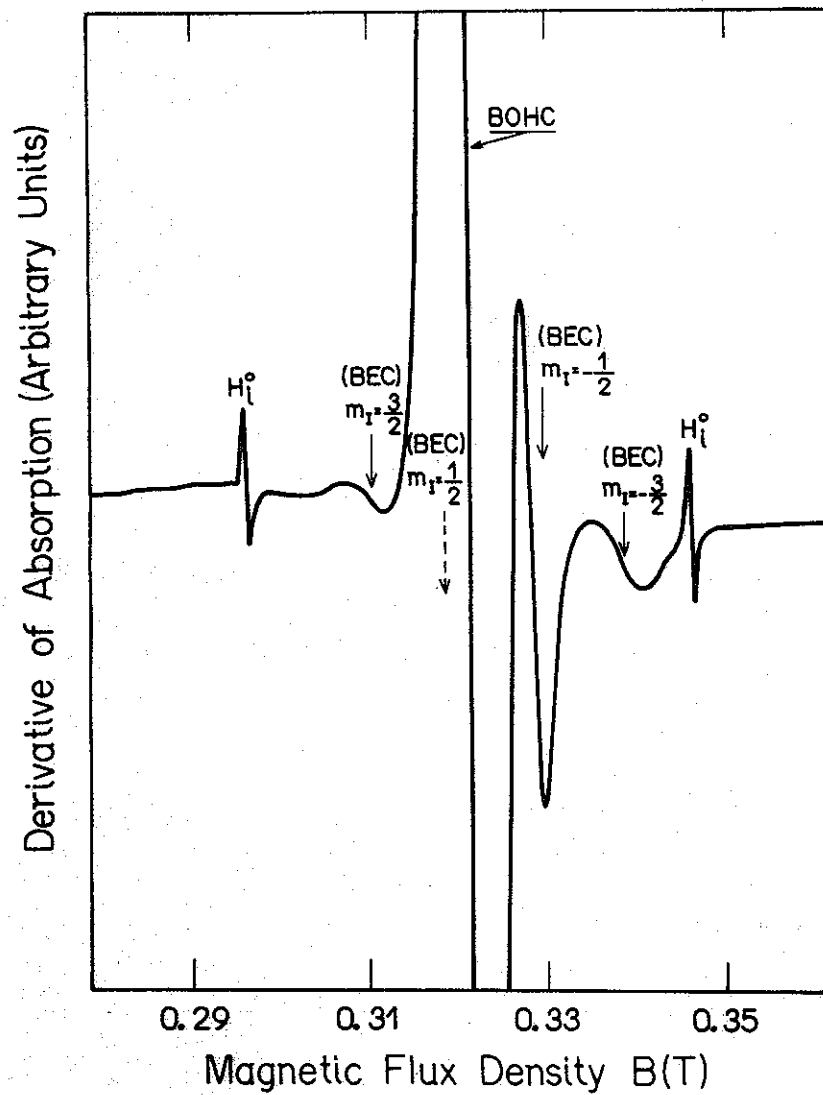


Fig. 2

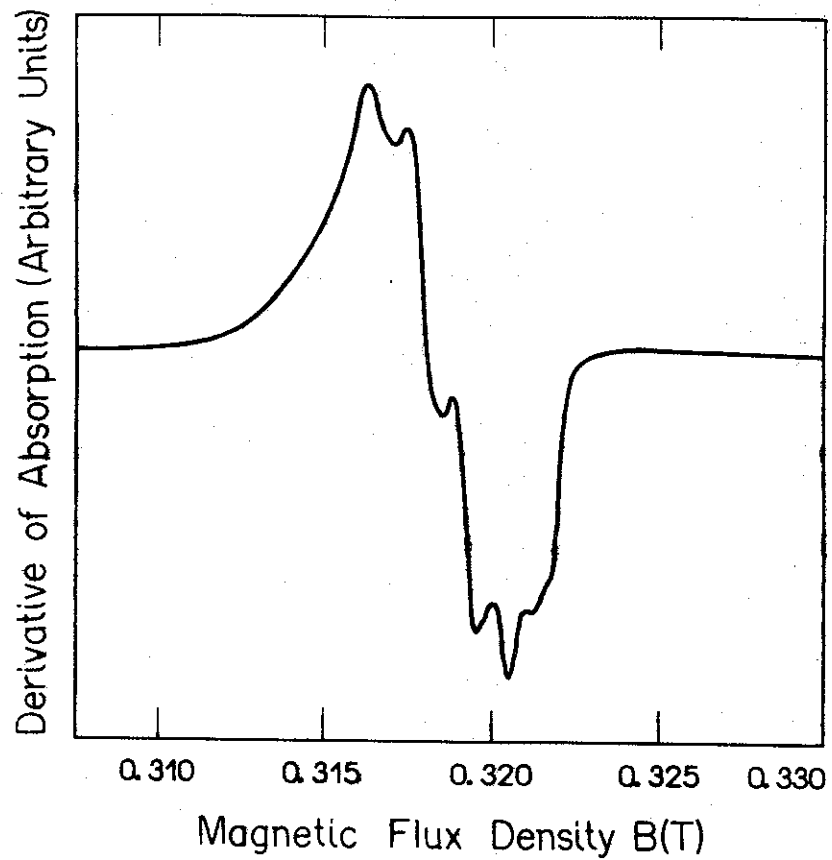


Fig. 3

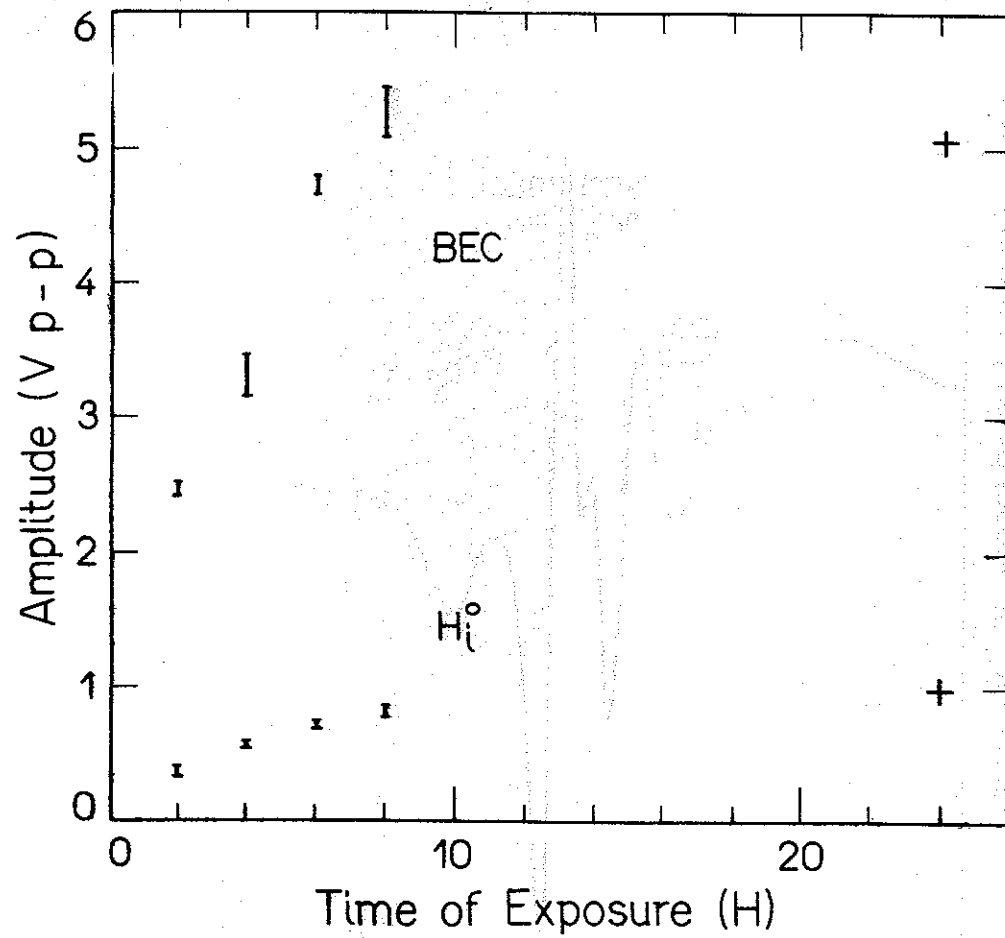


Fig. 4

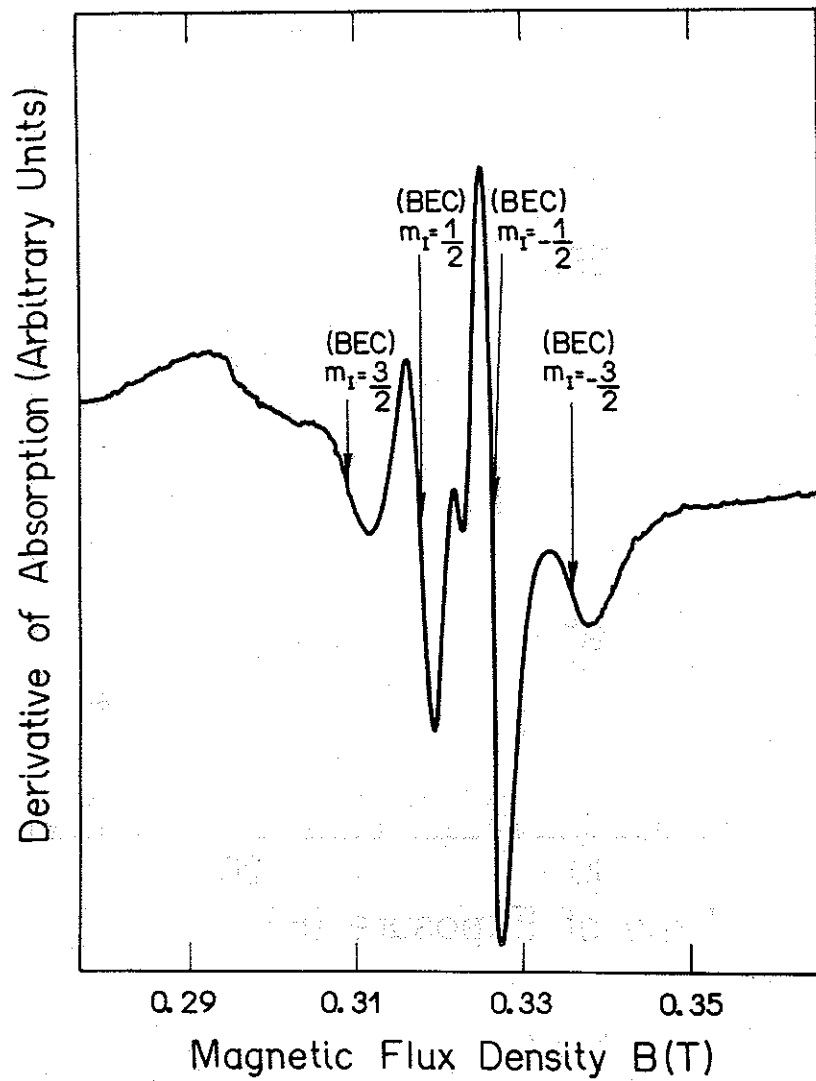


Fig. 5

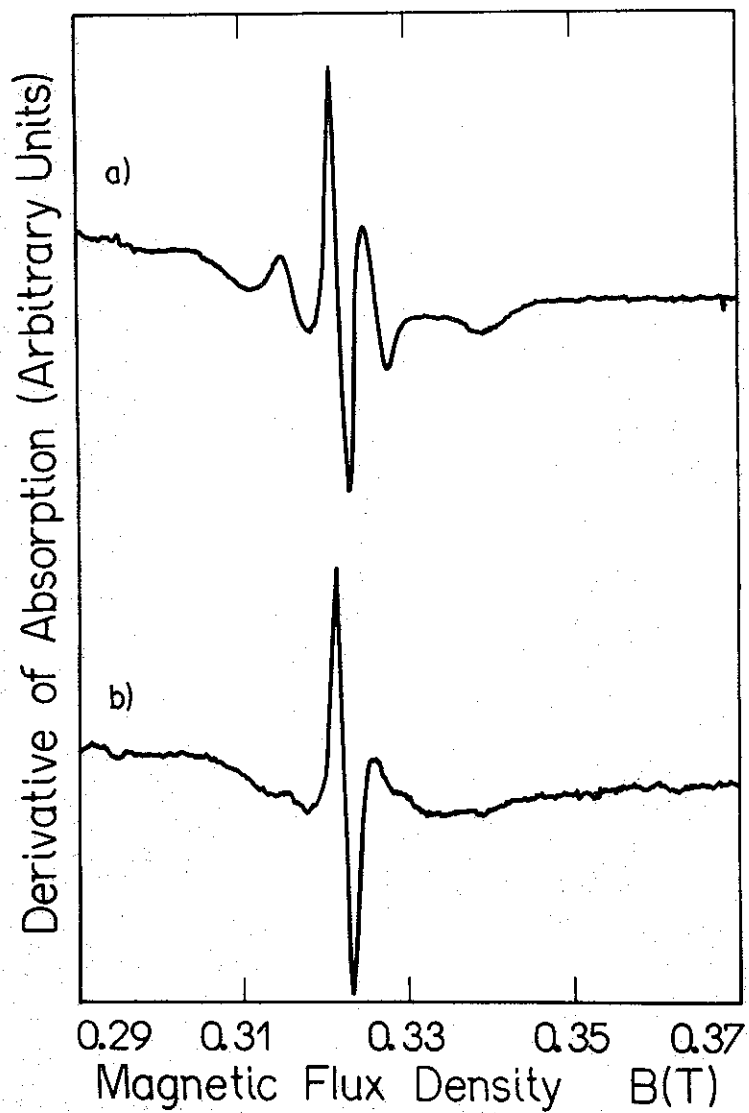


Fig. 6